Journal of Energetic Materials
Publication details, including instructions for authors and subscription information:
http://www.informaworld.com/smpp/title~content=t713770432

Three-dimensional modeling of inert metal-loaded explosives

Charles L. Mader[a]; James D. Kershner[a]; George H. Pimbley[a]
[a] Los Alamos National Laboratory, Los Alamos, New Mexico, (USA)

To cite this Article Mader, Charles L. , Kershner, James D. and Pimbley, George H.(1983) 'Three-dimensional modeling of inert metal-loaded explosives', Journal of Energetic Materials, 1: 4, 293 — 324
To link to this Article: DOI: 10.1080/07370658308012323
URL: http://dx.doi.org/10.1080/07370658308012323

THREE-DIMENSIONAL MODELING OF INERT METAL-LOADED EXPLOSIVES

by

Charles L. Mader, James D. Kershner, and George H. Pimbley
Los Alamos National Laboratory
Los Alamos, New Mexico 87545 (USA)

ABSTRACT

The reactive three-dimensional hydrodynamic code 3DE has been used to investigate the reactive hydrodynamics of a matrix of tungsten particles in HMX. A propagating detonation proceeding through the matrix of tungsten particles gives calculated detonation velocities and pressures that are much higher than observed. If the heterogeneous shock initiation Forest Fire rate for HMX is used to describe the reactive kinetics, some of the individual detonation wavelets between the tungsten particles fail. The shocked explosive continues to decompose and release energy after shock passage.

Equations of state are described for a tungsten and a lead-loaded explosive that reproduce the observed performance of these nonideal explosives. The calibrated equations of state use a partial energy release suggested by the three-dimensional model. Evidence is presented that the explosives have a flat top Taylor wave characteristic of weak detonations.

Journal of Energetic Materials Vol. 1, 293-324 (1983)

Published in 1983 by Dowden, Brodman & Devine, Inc.

INTRODUCTION

The addition of tungsten or lead to HMX or RDX results in a nonideal explosive. A nonideal explosive as defined in Ref. 1 is an explosive having a C-J pressure, velocity, or expansion isentrope significantly different from those expected from equilibrium, steady-state calculations such as BKW. It has been observed[1-3] that the difference between the calculated and observed detonation pressure increases with increased metal concentration while the detonation velocity is adequately reproduced by the calculations. The depth of the dent in the plate dent experiment[4] is much greater for tungsten or lead-loaded explosives than expected for their observed detonation pressure. For example, a 60/30/10 volume percent RDX/Pb/Exon at 4.6 mg/mm^3 has a detonation pressure of 150 kbar as determined by metal plate acceleration data[1] and 345 kbar as determined by the plate dent vs C-J pressure correlation described in Ref. 4. The experimentally measured detonation velocity is 5.012 mm/μs. The BKW-calculated C-J pressure is 270 kbar and velocity is 5.096 mm/μs. Similar calculated results[1] are obtained whether the lead is considered as compressible or incompressible and whether the lead is in temperature and pressure equilibrium with the detonation products or in pressure equilibrium alone.

The purpose of this study was to examine the reactive fluid dynamics of a detonation interacting with a matrix of metal particles to determine the nature of the observed nonideal behavior.

MODELS ASSUMING PROPAGATING DETONATION BETWEEN PARTICLES

Al'tschuler[2] attributed the nonideal behavior of his tungsten-loaded HMX explosives to the explosive detonating at an average velocity determined by the individual detonation wavelets traveling around the metal particles. Dremin[5] attributed the nonideal behavior to a transfer of detonation product energy to the tungsten particles by heat conduction.

A one-dimensional model of layers of explosive and metal with dimensions appropriate to the size of the metal particles was considered. For the explosive system of HMX and W, the C-J pressure of HMX is 395 kbar and velocity is 9.159 mm/μs. The HMX detonation will interact with a tungsten plate forming a shock of 668 kbar and 830 K, moving at 4.95 mm/μs. A 65/35 volume percent HMX/tungsten system in layers would have a velocity of about 7.7 mm/μs. This velocity is much higher than the experimental value of 5 mm/μs.

To examine the Al'tschuler and Dremin proposals, we used the reactive hydrodynamic code called 3DE.[6] It has been used to study the interaction of multiple detonation waves[7] and the basic processes in shock initiation of heterogeneous explosives.[8]

Three-dimensional calculations of a detonation wave in HMX interacting with a matrix of particles showed the detonation wave propagating between the particles at the C-J detonation velocity with the actual velocity determined by the shortest path through the particles. This effective velocity was less than the HMX

detonation velocity and greater than the one-dimensional layer model velocity discussed earlier. The explosive shock pressures were C-J or even higher from the shock interaction with the tungsten and colliding detonation waves.

To demonstrate the detailed flow resulting from an HMX detonation wave interacting with a tungsten prism, the pressure contours for cross sections through the center of the prism are shown in Fig. 1. The three-dimensional computational grid contained 19 by 19 by 32 cells, (called I, J, K for the number of cells in the X, Y, and Z directions) each 0.01 mm on a side. The tungsten prism was described with 11 by 11 by 6 cells. The explosive burn was described by an Arrhenius rate law; however, identical results were obtained using the C-J burn technique.[1] A detonation wave of 395 kbar proceeds at 9.16 mm/μs through the HMX and interacts with the tungsten prism. A reflected shock proceeds back into the detonation products and a shock wave passes through the tungsten. The detonation wave travels around the tungsten prism and collides above the prism with pressures in excess of 800 kbar. The shock wave passing through the tungsten arrives at the upper interface about when the detonation wave collision occurs.

An identical calculation was performed permitting heat conduction between the detonation products and the shock-heated tungsten prism. The heat conductivity used for tungsten was 0.1 cal/cm-sec-deg-K and for the detonation products was 0.001 cal/cm-sec-deg-K. An insignificant amount of energy was trans-

ferred to the tungsten from the detonation products by heat conduction. The conductivity constants were increased by a factor of 100 and still a negligible amount of energy was transferred.

So the Al'tschuler and Dremin proposals do not describe the observed nonideal behavior of tungsten-loaded explosives because the velocities and pressures are much larger than observed. Models that assume propagating detonation between particles do not describe the observed nonideal behavior.

Let us consider a well characterized tungsten-loaded HMX explosive called X0233. The explosive consists of 55/34/11 volume percent of HMX/W/polystyrene and DOP. Its density is 7.41 mg/mm^3. The tungsten particle sizes are 70% coarse (0.02-0.04-mm diameter), 22.4% medium (0.005-0.015 mm) and 7.5% fine (0.0015-0.005 mm). So the tungsten particle size ranges over an order of magnitude. For this study we will consider a matrix of tungsten particles approximately 0.02 mm in diameter. The detonation velocity measured by W. Campbell[9] was 4.640 mm/μs and the detonation pressure from the aquarium test is 160 kbar as measured by S. Goldstein.[9] The steel plate dent depth for a 41.275-mm-diameter cylinder of X0233 is 8.53 mm, as measured by M. Urizar,[9] which corresponds to a detonation pressure of 297 kbar.[4] The BKW-calculated C-J performance is 277 kbar, 4.51 mm/μs, and 2015 K. This explosive exhibits the typical nonideal behavior.

Assuming the tungsten particles are located on a hexagonal close-packed lattice (HCP) and have a radius of 0.02 mm, the

closest distance between tungsten spheres is 0.0114 mm for 35-volume-percent tungsten in HMX. If the tungsten sphere radius is 0.03 mm, the closest distance between spheres is 0.0170 mm.

For 15-volume-percent tungsten in HMX, the tungsten spheres with a radius of 0.0133 mm are 0.0187 mm apart. If we increase the particle radius by a factor of 4 to 0.0532, the spheres are 0.0748 mm apart.

For 5-volume-percent tungsten in HMX, the tungsten spheres with radius of 0.0133 mm are 0.0388 mm apart.

We shall investigate the possibility that detonations cannot propagate in three-dimensional geometries with these dimensions.

MODELS PERMITTING FAILURE OF PROPAGATING DETONATION

The heterogeneous shock initiation burn model called Forest Fire[1] has been used to calculate failure of propagation of detonation as a function of diameter, pulse width of initiating shock, wave curvature, and changes in geometry such as turning corners. These are all dominated by the heterogeneous shock initiation mechanism. We assumed that the propagation or failure of detonation in a matrix of tungsten particles in HMX is likewise determined by the heterogeneous shock initiation process and described by the Forest Fire model. The Forest Fire rate for PBX 9404, described in Ref. 1, was used to describe the HMX in the matrix of explosive and tungsten.

The first question we need to answer is how does the failure radius of HMX change with confinement. Calculations were performed using the 2DL and 2DE codes with Forest Fire to determine the failure radius of HMX and the TATB-based shock insensitive explosive PBX 9502. The technique and constants used were identical to those described in Ref. 1. As shown in Table I, the calculated failure radius decreases by a factor of 5 as the density of the confinement increases to that of tungsten. The failure diameter of a cylinder of HMX confined by tungsten is about 0.1 mm. This is larger than the distance between tungsten particles in X0233 so it is possible for detonation to fail to propagate between the tungsten particles; however, the actual behavior of the detonation wavelets in the three-dimensional matrix must be calculated.

TABLE 1. Failure Radius

Confinement	Calculated Radius (mm)	Experimental (mm)
HMX		
Air	0.6 - 0.4	0.6 ± 0.1
Plexiglas	0.4 - 0.3	
Al	0.3 - 0.2	
W	0.1 - 0.05	
PBX 9502		
Air	5.0 - 4.0	4.5 ± 0.5
Plexiglas	4.0 - 3.0	
Al	3.0 - 2.0	
W	1.5 - 0.5	

5% Tungsten/95% HMX

Figure 2 shows the density and mass fraction cross-section contours for a matrix of 5% by volume tungsten in HMX. The computational grid contained 20 by 27 by 51 cells, each 0.00667 on a side. The tungsten spheres had a radius of 0.0133 mm and were described by 4 cells per sphere diameter. Numerical tests with 2 to six cells per sphere diameter showed the results were independent of grid size for more than 3 cells per sphere diameter. The closest distance for the HCP matrix between tungsten spheres was 0.0388 mm. The detonation starts to fail as it passes around the tungsten particles (shown by the mass fraction contours becoming farther apart), but complete decomposition occurs before the shock wave proceeds ahead of the reaction region.

15% Tungsten/85% HMX

Figures 3 and 4 show the density and mass fraction cross-section contours for a matrix of 15% by volume tungsten in HMX. Figure 3 shows the flow for tungsten spheres of 0.0133 mm. The closest distance for the HCP matrix between tungsten spheres was 0.0187 mm. The computational grid contained 14 by 19 by 43 cells, each 0.00667 mm on a side. The tungsten spheres were described by 4 cells per sphere diameter. Some of the detonation wavelets fail to propagate and the shock wave proceeds ahead of the reaction zone in regions of the flow. These partially reacted regions continue to decompose relatively slowly with time.

To demonstrate the effect of particle size, we increased the tungsten sphere radius by a factor of 4. Figure 4 shows the flow for tungsten spheres of 0.0532 mm. The closest distance for the HCP matrix between tungsten spheres was 0.0748 mm. This is close to the failure diameter of tungsten-confined HMX of 0.2 to 0.1 mm, so most of the HMX in the matrix is large enough to be above the failure diameter. The computational grid contained 14 by 19 by 43 cells, each 0.0267 mm on a side. The tungsten spheres were described by 4 cells per sphere diameter. In contrast to the previous case, most of the detonation wavelets pass around the tungsten particle without exhibiting failure. The shock wave proceeds along with the reaction region.

35% Tungsten/65% HMX

Figure 5 shows the density and mass fraction cross section for a matrix of 35% by volume tungsten in HMX. The computational grid contained 16 by 22 by 46 cells, each 0.00667 mm on a side. The tungsten spheres had a radius of 0.02 mm and were described by 6 cells per sphere diameter. The closest distance for the HCP matrix between tungsten spheres was 0.0114 mm. Many of the detonation wavelets fail to propagate and the shock wave proceeds ahead of the reaction zone. These partially reacted regions continue to decompose with time.

Conclusions

The nonideal behavior of inert metal-loaded explosives can be attributed to failure of the individual detonation wavelets as

they pass between the tungsten particles. The shocked, partially decomposed explosive continues to decompose and release energy relatively slowly after shock passage.

The effect of increased concentration of inert metal is to reduce the distance between particles, resulting in more detonation wavelets failing and lower detonation pressures in the explosive.

The effect of larger particle size of inert metal is to increase the distance between particles, resulting in less detonation wavelets failing and higher effective pressures in the explosives. This effect of particle size is in agreement with the experimental results of Dremin.[5]

The expansion isentrope of the inert metal-loaded explosive must be less steep than for completely reacted ideal explosives of the same detonation pressure since additional decomposition occurs behind the detonation shock front. The high pressure expansion isentrope would result in larger plate dents and greater aquarium bubble expansions than those characteristic of ideal explosives with the same detonation pressure.

APPLICATION TO X0233

The three-dimensional model for the nonideal behavior of tungsten-loaded HMX indicates that the observed low detonation pressure results from failure of some of the individual detonation wavelets. The explosive continues to decompose and release energy after shock passage.

The BKW equation of state represents the ideal behavior of explosive mixtures if all the explosive detonates. The gamma-law equation of state through the experimental detonation pressure and velocity represents the behavior if no additional energy is released behind the detonation front. To a first approximation, we can account for the energy actually present during expansion of the detonation products by passing the BKW isentrope through the detonation Hugoniot pressure corresponding to the experimental detonation pressure. If the shock velocity is sufficiently close to the detonation velocity, the resulting BKW isentrope should closely approximate the expansion behavior of the detonation products after complete decomposition has occurred behind the detonation front. For X0233, the shock velocity at 160 kbar on the detonation product Hugoniot is too high. The detonation Hugoniot must include the fact that a significant amount of explosive is not initially decomposed. This was accomplished by increasing (more negative) the heat of formation of the explosive by 47.4 calories per gram of explosive. The energy was returned to the detonation product isentrope in increments of 4.75 calories per gram per isentrope interval of 0.8 times the pressure. The resulting isentrope was insensitive to either the increment or interval details.

The gamma-law and BKW isentrope through the experimental detonation state are shown in Fig. 6. Calculations of the plate dent using the 2DE code and technique described in Ref. 1 for the

three X0233 equations of state are shown, along with the experimental plate dent, in Table 2.

The BKW equation of state through the experimental detonation state reproduces the experimental detonation pressure of 160 kbar, the velocity, and the plate dent that is characteristic of an ideal explosive detonation pressure of 297 kbar. We shall further test our description of the explosive equation of state by comparing with the experimentally observed behavior of the expansion of the detonation products and shock wave in water.

The aquarium test was performed by S. Goldstein.[9] Calculations of the aquarium test for a 20.63-mm radius cylinder of X0233 in water were performed using the 2DL code[1] and the experiments were performed as described in Refs. 1 and 10.

TABLE 2. X0233 Plate Dents

Equation of State	Calculated Dent (mm)	Experimental Dent (mm)
BKW ideal	11.0	8.53
Gamma law	5.0	
BKW through experimental detonation state and energy returned to isentrope	9.0	

The photograph, taken by S. Goldstein with the image intensifier camera, of the shock wave in water and the interface between the detonation products and water is shown in Fig. 7. The interface between the water and the detonation products is much more ragged than observed previously for more ideal explosives. This can be interpreted as evidence of irregular decomposition of the explosive, in agreement with our proposed failure of some of the individual detonation wavelets between the tungsten particles and later decomposition of the explosive in these regions.

The calculated and experimental shock wave and detonation product/water interface are shown for the gamma-law equation of state in Fig. 8, the BKW ideal equation of state in Fig. 9, and in Fig. 10 the BKW equation of state through the experimental detonation state with the energy returned to the isentrope. This BKW equation of state reproduces the experimental shock wave and detonation product interface positions. The equation of state constants for X0233 are given in Table 3. The constants have the same identity as described in Ref. 1.

To model the explosive performance of X0233, it is necessary to displace the BKW detonation product Hugoniot so that it intersected the observed detonation pressure and velocity by decreasing the energy available to the detonation products.

The detonation is programmed to travel with the experimental detonation velocity using either the sharp-shock burn[1] or the volume burn.[1] The velocity or specific volume at the detonation

state is larger than the C-J state values for the detonation product Hugoniot passing through the detonation state. This results in what we call a weak detonation with the one dimensional pressure-distance profile shown in Fig. 11. The detonation products behind the detonation front cannot reach the C-J state since the wave is traveling faster than a C-J detonation. A flat top Taylor wave forms behind the detonation front.

To further test the weak detonation model, S. Goldstein measured the water shock velocity in the aquarium test after the detonation wave interacted with the water above the top of the X0233 cylinder. Her experimental water shock velocities, as a function of distance above the top of the explosive cylinder, are shown in Fig. 12 along with the calculated water shock velocities. They are consistent with a flat top Taylor wave characteristic of a weak detonation and a detonation front pressure of 160 kbars. The initial water shock velocities exhibit behavior characteristic of irregular decomposition of the explosive near the shock front. The calculated pressure contours are shown in Fig. 13.

The displaced BKW isentrope that will describe the observed plate dent, aquarium water shock profiles, explosive interface, and the detonation velocity of X0233 exhibits a weak detonation behavior.

APPLICATION TO RDX/EXON/Pb

In Ref. 1, the explosive mixture 60/10/30 by volume of RDX/Exon/Pb was described. It has a density of 4.60 mg/mm^3, a detonation velocity of 5.0 mm/μs, and a detonation pressure determined

from aluminum plate push experiments of 150 kbar. The experimental plate dent of 10.23 mm corresponds to a detonation pressure of 346 kbar. The BKW-calculated C-J performance is 270 kbar, 5.096 mm/μs, and 2242 K. This is the most nonideal inert metal-loaded explosive known to the authors. The very small particle size of the lead powder used results in failure of many individual detonation wavelets as they pass between the lead particles.

To account for the nonideal behavior, it is insufficient to just displace the BKW isentrope through the detonation product Hugoniot at 150 kbar because the shock velocity of 6.875 mm/μs is much higher than the experimental velocity of 5.0 mm/μs. The detonation product shock Hugoniot must include the fact that a significant amount of explosive is not initially decomposed. This was accomplished by increasing the heat of formation (more negative) of the explosive mixture until the shock velocity at 150 kbar on the detonation product Hugoniot agreed with the observed detonation velocity. This required increasing the heat of formation by 183 calories per gram of explosive mixture. An isentrope through this Hugoniot state was too weak to reproduce the observed plate dent so the energy was returned to the detonation product isentrope in increments of 20 calories per gram per isentrope interval of 0.8 times the pressure. The resulting isentrope was insensitive to the increment or interval details. The technique is similar to that used to describe ANFO in Refs. 1 and 10. The resulting isentropes with and without energy returned are shown in

Fig. 14, along with the ideal BKW isentrope and the gamma-law isentrope through the C-J state. The BKW equation of state constants for the isentrope displaced through the experimental detonation pressure and velocity are given in Table 3. Calculations of the plate dent, using the 2DE code and technique described in Ref. 1 for the three equations of state, along with the experimental plate dent are shown in Table 4.

TABLE 3. Equation-of-State Constants

	X0233	RDX/Exon/Pb
A	-7.21312551798E+00	-6.25053662637E+00
B	-1.39485557915E+00	-1.95155050436E+00
C	2.23915871633E-01	-2.90284985132E-01
D	-1.77095802814E-01	-6.32661508840E-02
E	-1.23849736471E-02	-1.07335025294E-03
K	-2.12182312874E+00	-2.07715982237E+00
L	1.53002477916E-01	2.36461923017E-01
M	4.04717285191E-02	7.23556291125E-02
N	4.88663567104E-03	9.99231901764E-03
O	2.14785041504E-04	4.86763363442E-04
Q	6.97901236695E+00	7.01971398005E+00
R	-5.93317817321E-02	-1.39773676027E-01
S	-8.84798754816E-02	-2.27283819350E-01
T	-7.10719273057E-04	1.63850564686E-02
U	2.50870872978E-02	5.34425309797E-02
C_V'	0.5	0.5
Z	0.1	0.1
P_{CJ}	0.24156	0.21056
D_{CJ}	4.310	4.745
V_{CJ}	0.113	0.17319
P*	0.16000	0.15000
D*	4.688	5.007
V*	0.121698	0.1891

*Displaced Values

The BKW equation of state through the experimental detonation state with the energy returned to the isentrope reproduces the experimental detonation pressure of 150 kbar and velocity of 5.0 mm/μs and the plate dent characteristic of an ideal explosive detonation pressure of 346 kbar. It exhibits weak detonation behavior similar to that observed in X0233.

TABLE 4. 60/10/30 RDX/Exon/Pb Plate Dents

Equation of State	Calculated Dent (mm)	Experimental Dent (mm)
BKW ideal	12.0	10.24
Gamma law	5.0	
BKW through experimental detonation state	9.0	
BKW through experimental detonation state and energy returned to isentrope	10.0	

CONCLUSIONS

The nonideal behavior of inert metal-loaded explosives may be attributed to the failure of some of the individual detonation wavelets between the metal particles and the subsequent decomposition of the partially decomposed explosive behind the detonation front. The effect of composition and particle size has been modeled qualitatively.

Characterization of the explosive requires experimental determination of the detonation pressure and velocity. If the ex-

perimental state is near the ideal BKW detonation product Hugoniot, the isentrope of the detonation products can be determined by displacing the isentrope through the experimental state. Otherwise, the ideal detonation product Hugoniot must be displaced so that it intersects the observed detonation pressure and velocity by decreasing the energy available to the detonation products. This results in a weak detonation with a flat top Taylor wave.

The techniques give useful engineering descriptions for modeling the nonideal explosive performance, but must be carefully evaluated by comparing with experimentally determined performance data. We can model the isentropic behavior at low pressures, which previously has not been possible.

A useful conclusion from this study is the indication that the observed variation of performance with particle size of the inert material reported by Dremin[5] for a few explosive systems should be expected to occur for all inert metal-loaded explosives.

It should be possible to significantly change the time history of availability of the explosive energy by variations of the composition and particle size of the inert metal. A systematic experimental study of the explosive performance of an inert metal-loaded explosive with particle size would be a valuable addition to the explosive performance data base.

This study is an example of how a fundamental study of a complicated three-dimensional reactive flow problem can result in

sufficient increased understanding of the nature of the problem that a practicable engineering solution can be devised.

ACKNOWLEDGMENTS

The authors wish to recognize the contributions to the calculations described in this paper by their co-worker Allen L. Bowman. They also wish to recognize the experimental data furnished by Selma Goldstein, Wayne Campbell, Manuel Urizar, and Steve Harmony of the Los Alamos National Laboratory.

REFERENCES

1. Charles L. Mader, Numerical Modeling of Detonations, University of California Press, Berkeley, 1979.
2. L. V. Al'tschuler, V. T. Ryazonov, and M. P. Speranskava, "The Effect of Heavy Admixture on the Detonation Conditions of Condensed Explosive Substances," Zhurnal Prikladnov Mekhaniki i Tekhnicheskoy Fisiki, No. 1, 122 (1972).
3. I. M. Voskoboinikov, A. A. Kotomin, and N. F. Voskoboinikova, "The Effect of Inert Additives on the Velocity of Pushing Plates by Composite Explosives," Physics of Combustion and Explosion 18, 108 (1982).
4. Louis C. Smith, "On Brisance, and a Plate-Denting Test for the Estimating of Detonation Pressure," Explosivstoffe, No. 5, 6 (1967).
5. K. K. Shvedov, A. I. Aniskin, A. A. Il'in, and A. A. Dremin, "Detonation of Highly Dilute Porous Explosives, II Influence of Inert Additive on the Structure of the Front," Combustion, Explosion and Shock Waves 18, 64 (1982).

6. Charles L. Mader and James D. Kershner, "Three-Dimensional Modeling of Triple-Wave Initiation of Insensitive Explosives," Los Alamos Scientific Laboratory report LA-8206 (1980).

7. Charles L. Mader, Seventh Symposium (International) on Detonation, p. 335, Office of Naval Research (1981).

8. Charles L. Mader and James D. Kershner, "Three-Dimensional Modeling of Shock Initiation of Heterogeneous Explosives," Nineteenth Symposium (International) on Combustion, pp. 685-690 (1982).

9. Private communication, Los Alamos National Laboratory data.

10. J. N. Johnson, C. L. Mader, and S. Goldstein, "Performance Properties of Commercial Explosives," Propellants, Explosives, and Pyrotechnics 8, 8-18 (1983).

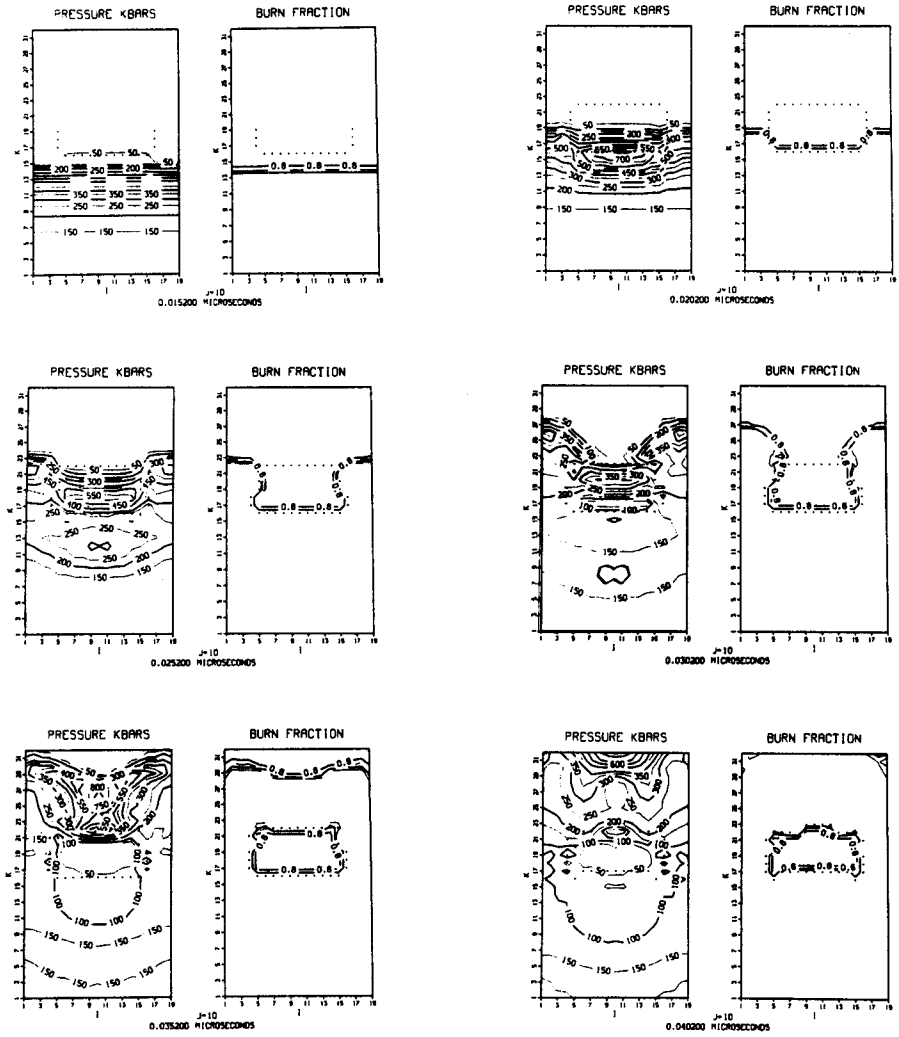

FIGURE 1

A 0.1- by 0.1- by 0.06-mm tungsten prism in 0.19 by 0.19 by 0.32 mm of HMX. The pressure contours for a cross section through 0.10 mm are shown at various times.

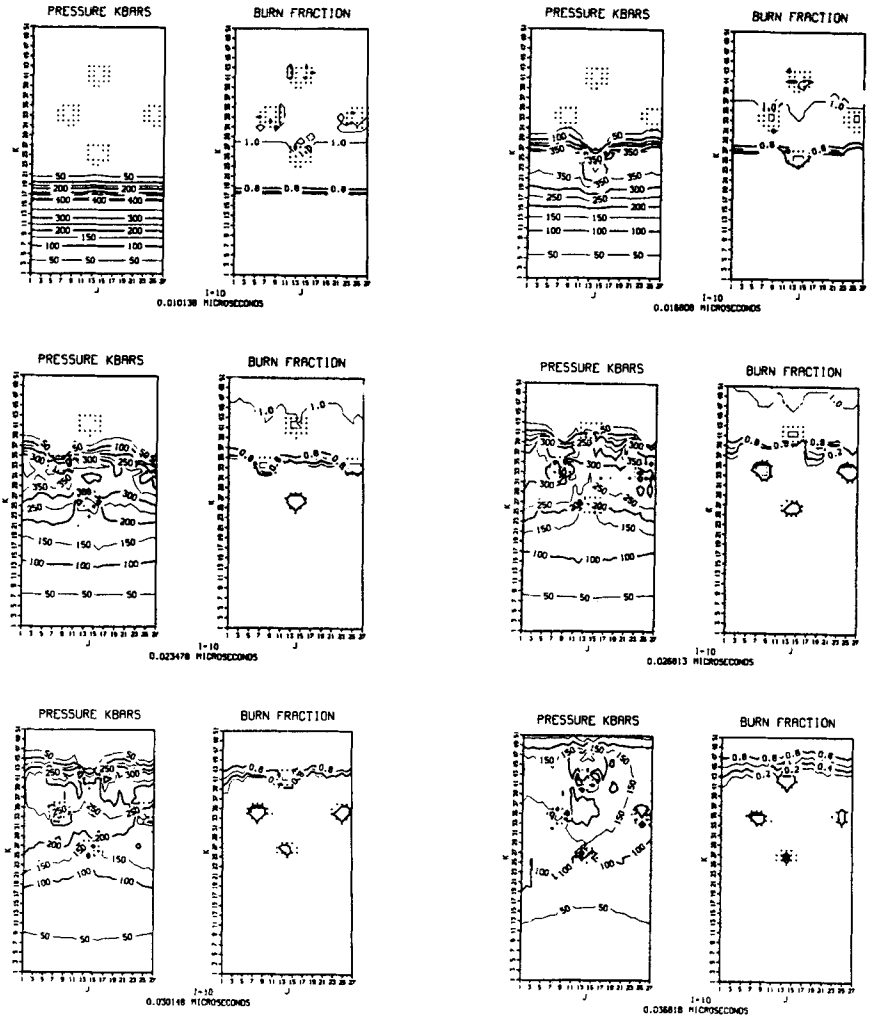

FIGURE 2
A matrix of 5% tungsten in HMX. The tungsten spheres have a 0.0133mm radius. The density and mass fraction contours are shown for a cross section at I = 10.

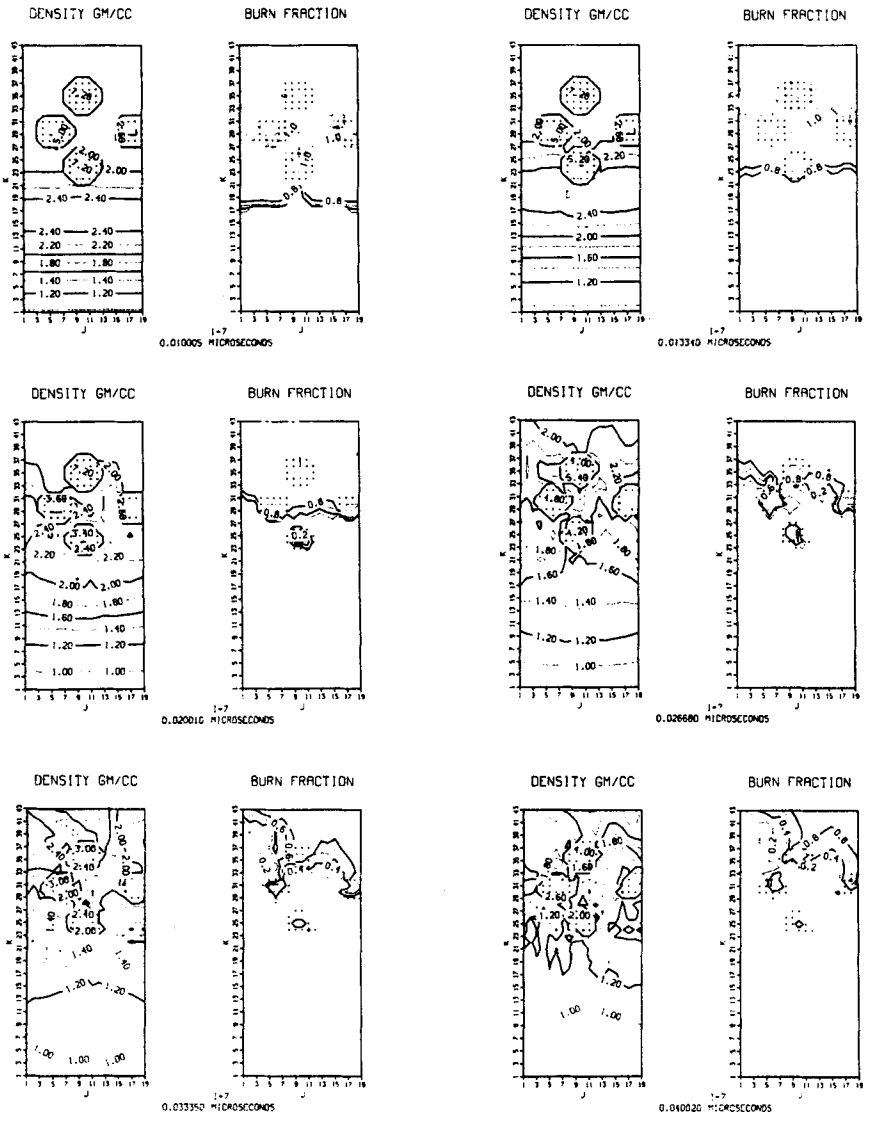

FIGURE 3
A matrix of 15% tungsten in HMX. The tungsten spheres have a 0.0133mm radius. The density and mass fraction contours are shown for a cross section at I = 7.

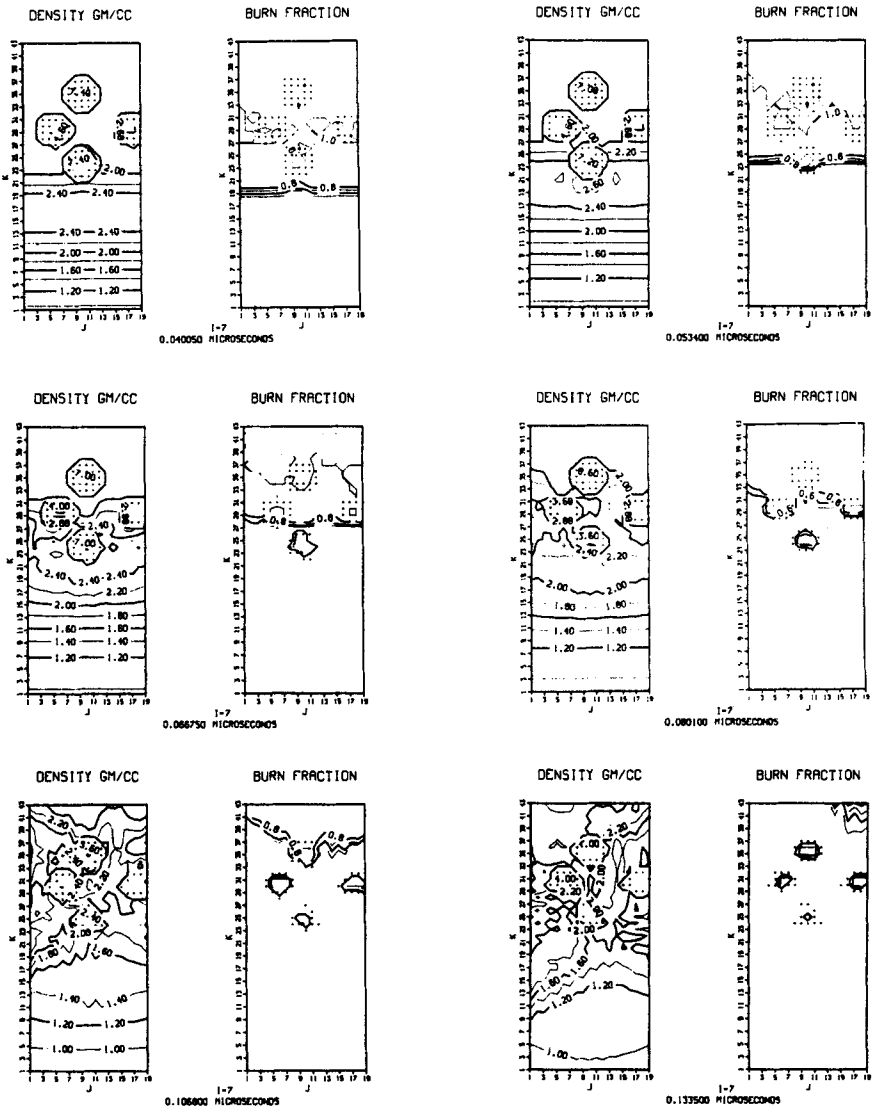

FIGURE 4
A matrix of 15% tungsten in HMX. The tungsten spheres have a 0.053 -mm radius. The density and mass fraction contours are shown for a cross section of I = 7.

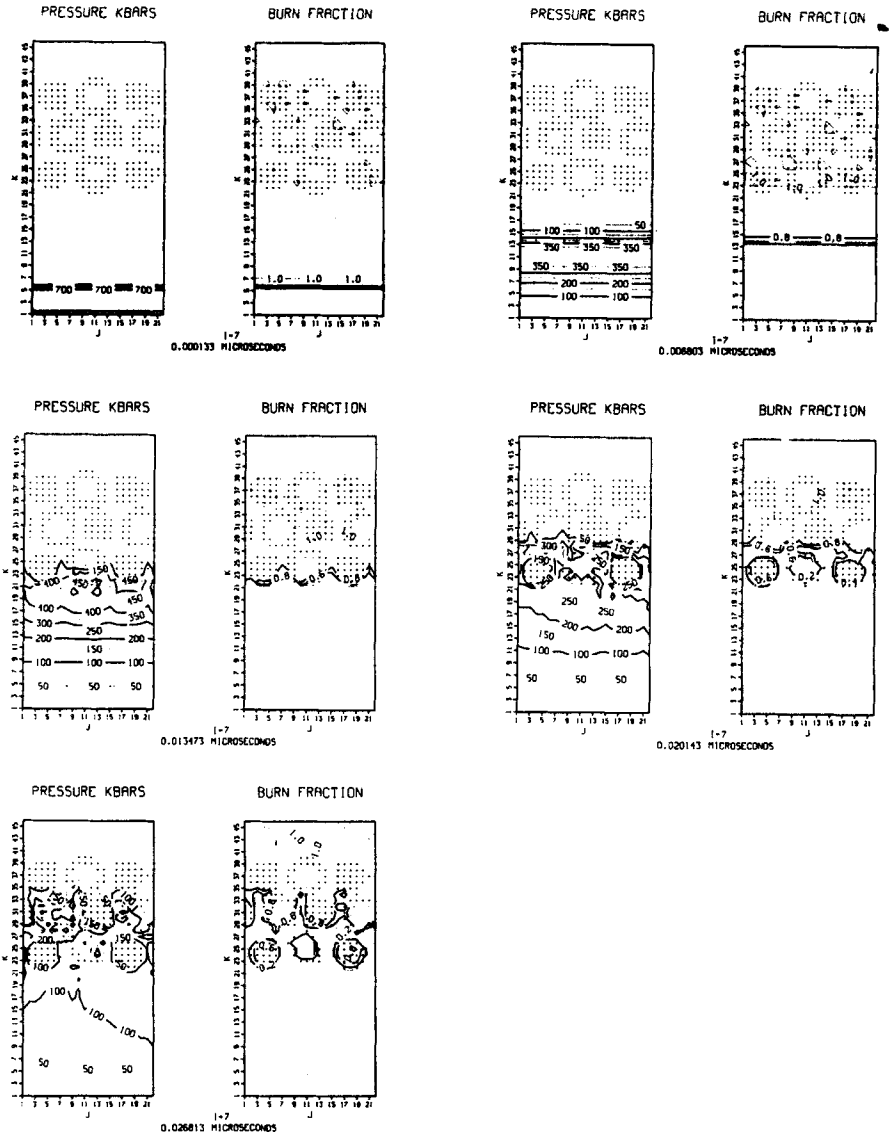

FIGURE 5
A matrix of 35% tungsten in HMX. The tungsten spheres have a 0.02-mm radius. The density and mass fraction contours are shown for a cross section of I = 7 .

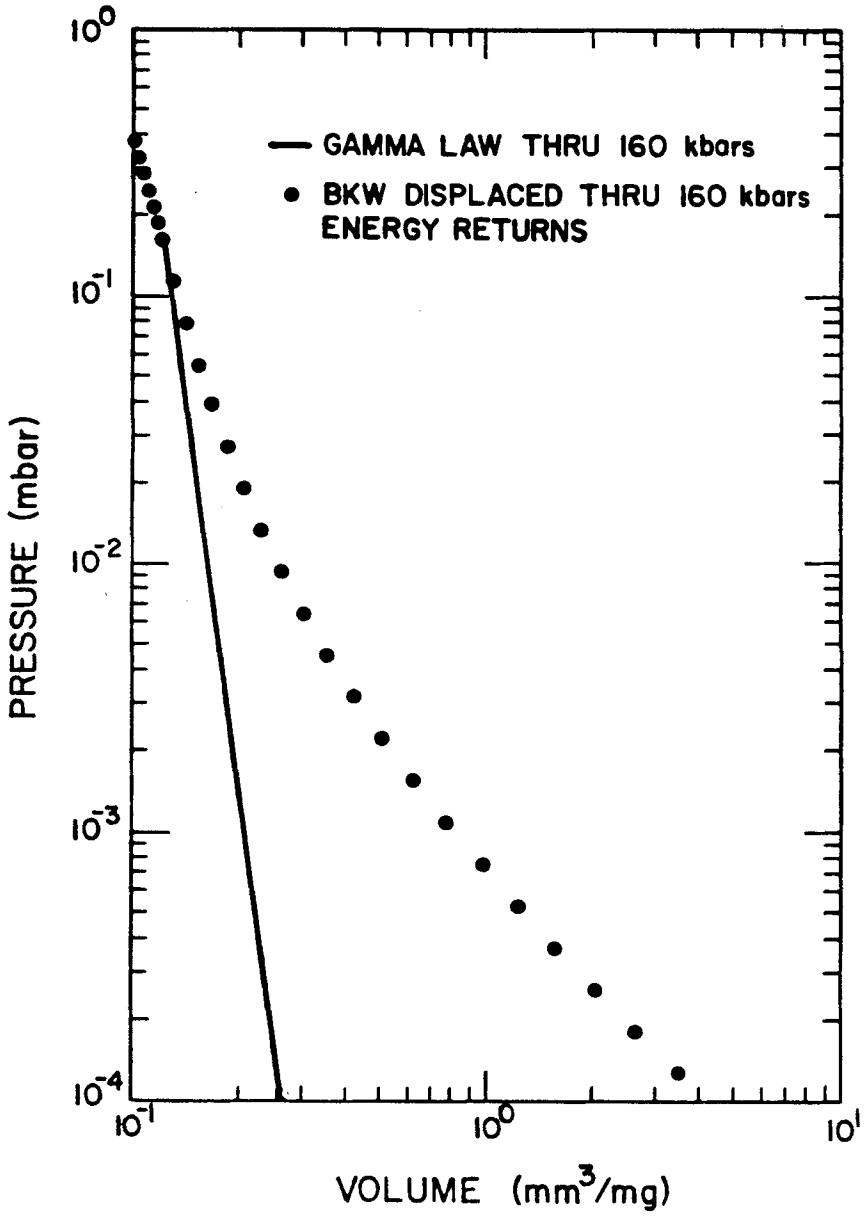

FIGURE 6
The X0233 gamma-law isentrope through the experimental detonation pressure and velocity, and the BKW isentrope through the experimental detonation pressure and velocity with the energy returned.

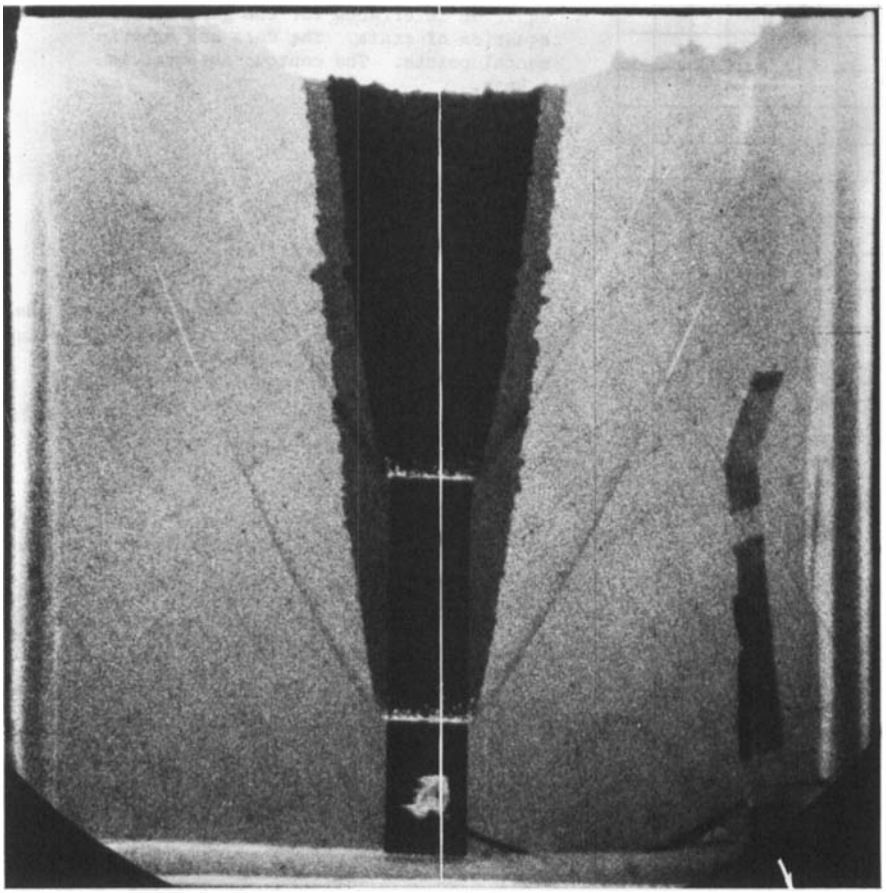

FIGURE 7
The aquarium test for X0233. Two photographic exposures taken with the image intensifier camera. The shock wave in the water and the interface between the detonation products and water are shown.

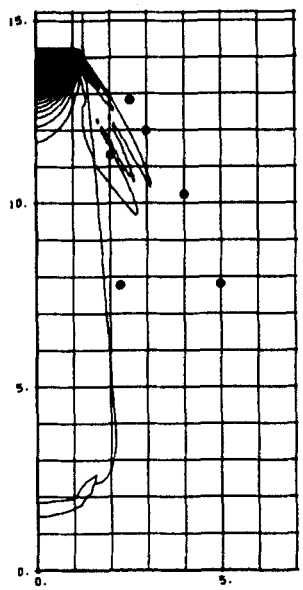

FIGURE 8
The experimental and the calculated X0233 aquarium interfaces for the gamma-law equation of state. The dots are experimental points. The contour interval is 5 kbar.

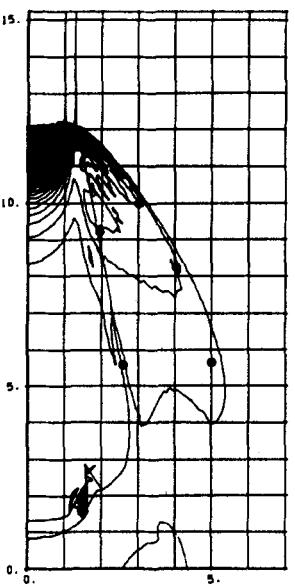

FIGURE 9
The experimental and the calculated X0233 aquarium interfaces for the BKW equation of state. The dots are experimental points. The contour interval is 5 kbar.

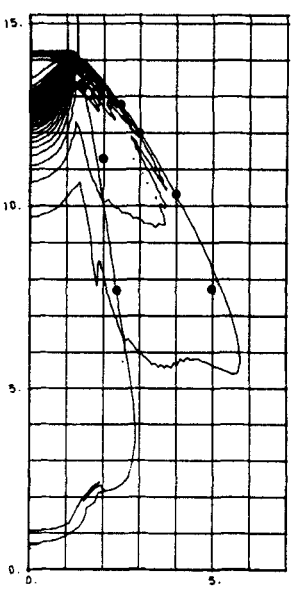

FIGURE 10
The experimental and the calculated X0233 aquarium interfaces for the displaced BKW equation of state. The dots are experimental points. The contour interval is 5 kbar.

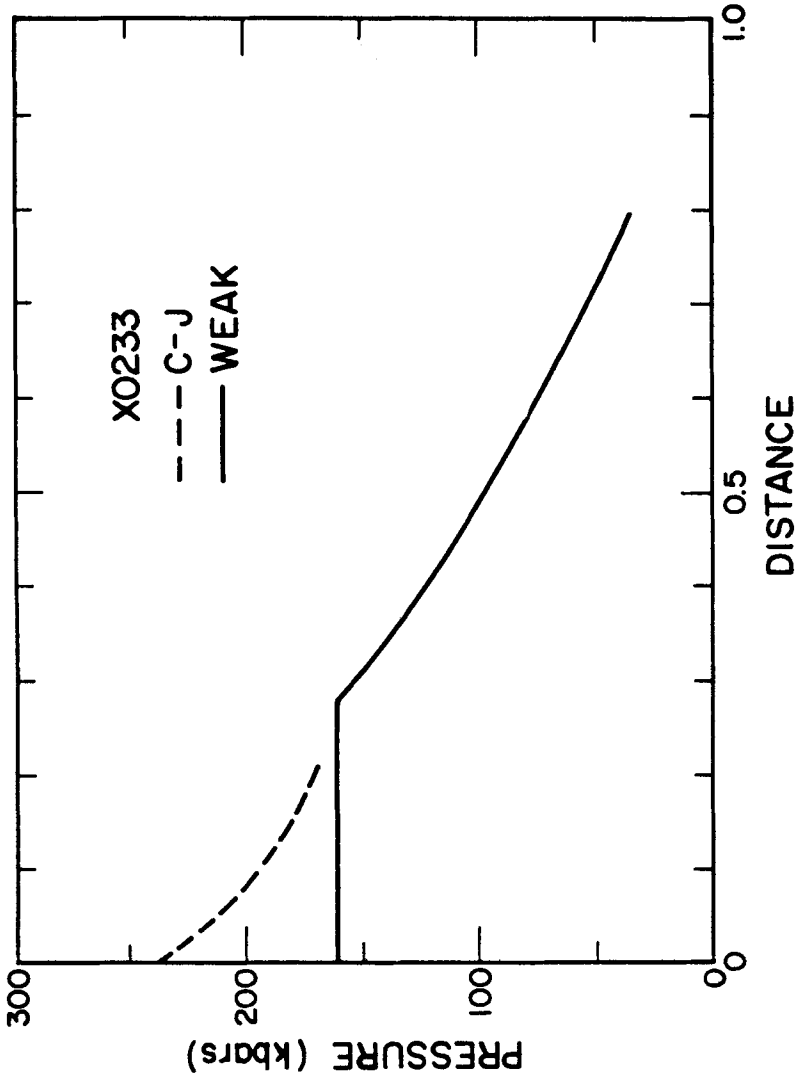

FIGURE 11
The Taylor waves for X0233 assuming a C-J and a weak detonation.

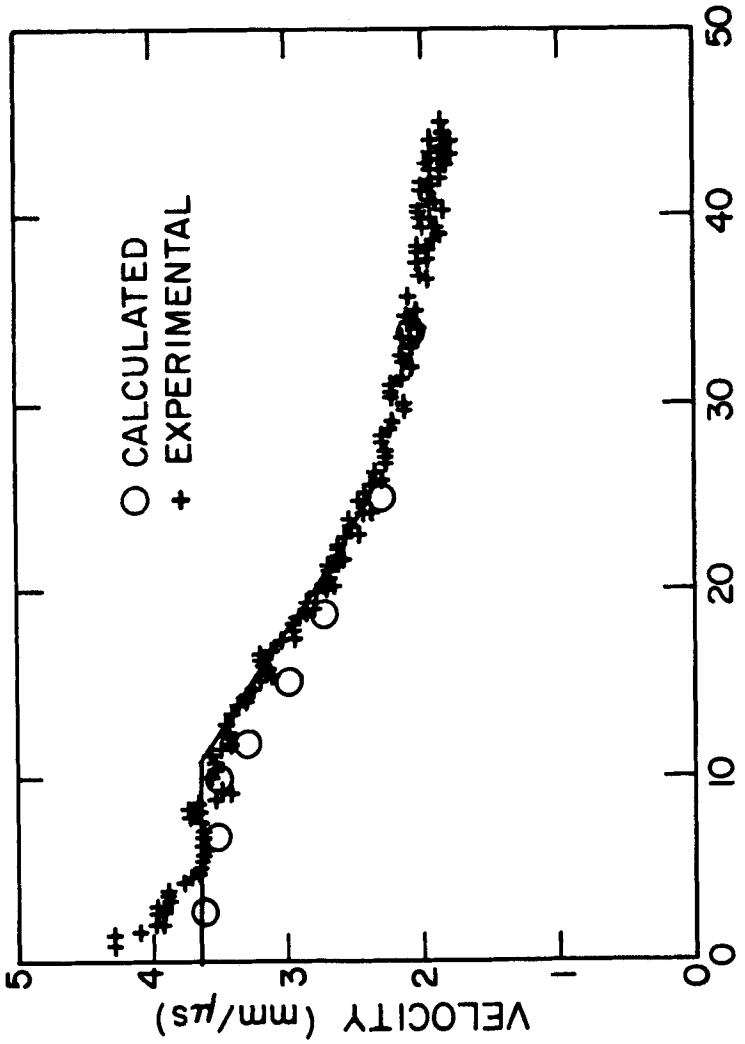

FIGURE 12
The calculated and experimental water shock velocities for the X0233 detonation front shocking water.

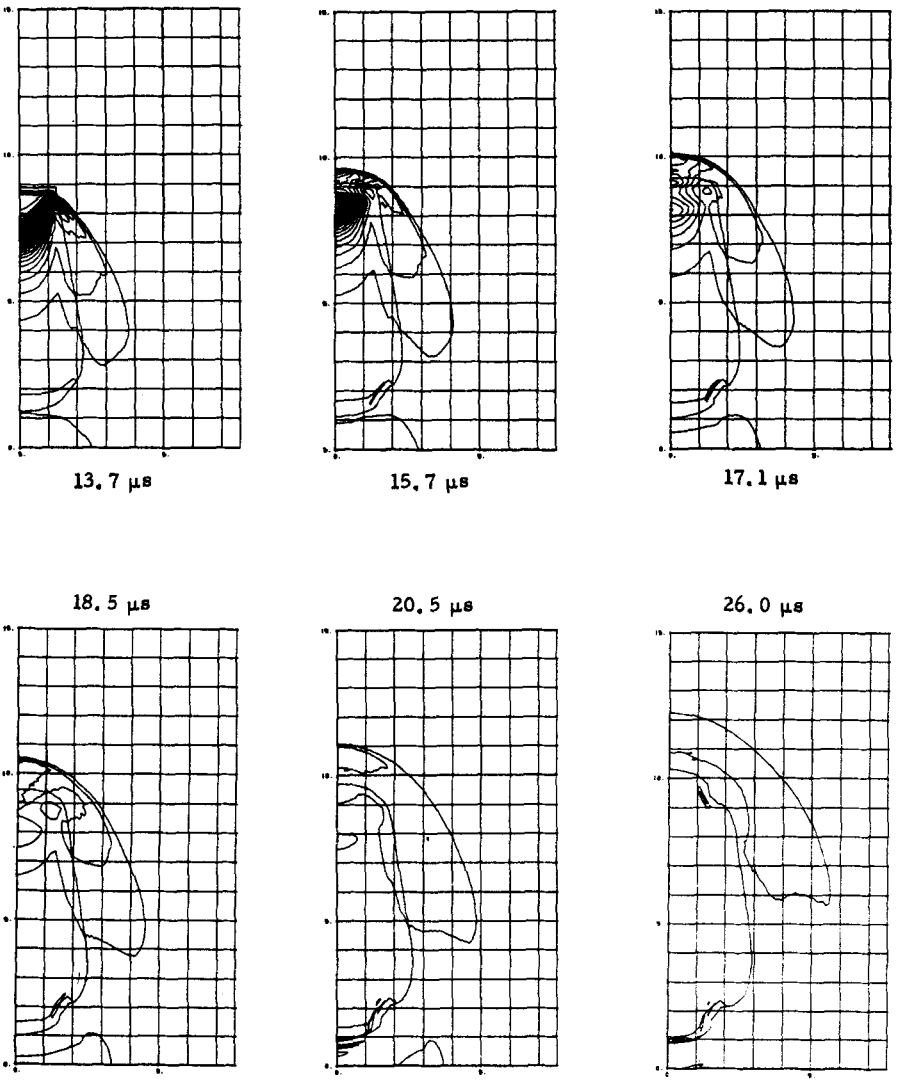

FIGURE 13
The calculated pressure contours for a cylinder of X0233 immersed in water. The contour interval is 5 kbar. The peak detonation pressure is 160 kbar. The weak detonation is shown by the region of no contours near the detonation front.

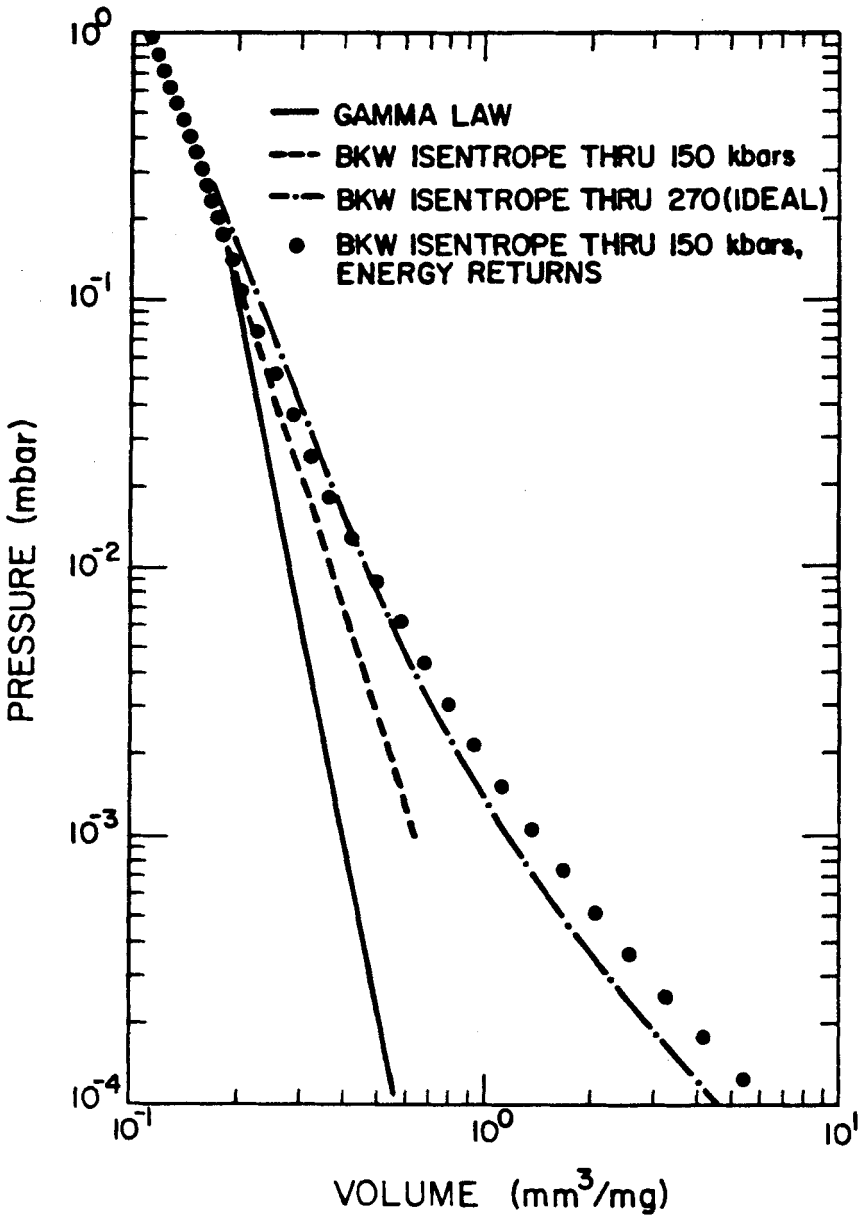

FIGURE 14
The 60/10/30 RDX/Exon/Pb BKW ideal isentrope, the gamma-law isentrope through the experimental detonation pressure and velocity, and the BKW isentrope through the experimental pressure and velocity with and without the energy returned.